LASER THOMSON SCATTERING DIAGNOSTICS -DEVELOPMENTS AND APPLICATIONS TO HIGH-TEMPERATURE PLASMAS AND PLASMAS FOR INDUSTRIAL APPLICATIONS

Katsunori Muraoka
School of Engineering, Chubu University, Kasugai, Aichi 487-8501, Japan

Laser Thomson scattering was applied to plasma diagnostics almost as soon as laser was invented in 1960. The most important contribution of the technique to plasma physics and controlled fusion came from the confirmation of good confinement of plasmas in the T-3 tokamak in 1968, by a collaboration of Russian and British physicists. Since then, extensive developments of the technique have been made to meet various measurement requirements, not only in high-temperature plasmas but in plasmas for industrial applications. In this article, these developments are briefly reviewed, followed by the work of the author and its implications for understanding various plasma phenomena.
PACS: 52.70.-m,52.70.Kz

1. INTRODUCTION

lthough the principle of laser Thomson scattering (LTS, here the author refers only to the incoherent region of laser Thomson scattering from plasmas [1]) has been known and used for diagnosing electron properties in plasmas for many years, ingenious developments for various applications have been necessary to meet requirements at each plasma and surrounding conditions. In this article, the author describes how these developments have been made worldwide and mentions his own experiences of measuring electron density and temperature, or more generally electron energy distribution function (eedf), in plasmas, for the last 35 years.

2. BRIEF SURVEY OF LTS

The principle and general experimental arrange-ment of LTS have been described in detail in various references, e.g. [1,2]. The author divides developments of LTS to *three stages*, as shown in Fig. 1.

The first stage is the development of LTS started by using a single-pulse ruby laser for high-temperature plasma studies in the middle of 1960's, and culminated in the confirmation of performance claimed for the T-3 tokamak in 1968 [3]. Refinements, such as TVTS (television Thomson scattering) [4] and LIDAR (light detection and ranging) Thomson scattering, [5] to meet the requirements of a very high spatial resolution and an optical access limitation, respectively, followed.

The second stage started in the late 1980s. Here, data accumulation has been of essence for plasmas having electron densities n_e below 10^{18} m^{-3}. This is because the scattered photon numbers, N_p, from a plasma having electron density of n_e are typically expressed as $N_p = 10^{-17} n_e$. Plasmas having n_e below 10^{18} m^{-3} were started to be used in industrial applications around 1980, and understanding of their electron properties was highly required then.

The third stage concerns the application of LTS to micro-discharge plasmas formed as close as 100 μm to a material surface and was prompted by the need to improve the efficiency of plasma display panels (PDPs) in particular. The suppression of stray light from the surface was of utmost importance, and a triple-grating spectrometer played an essential part here.

Each stage is still under developments to meet even higher measurement requirements and more and more stringent measuring environments. In this respect, specific examples from the work of the authors are described in detail.

3. THE FIRST STAGE LTS

The importance of LTS on the T-3 tokamak [3] can hardly be overstated in plasma physics in two senses; namely it had cleared the pessimism surrounding fusion researches in late '60 and has recently been culminated in the ITER project, while the other aspect was that plasma researchers in general recognized the usefulness and importance of laser diagnostics methods in general and many people started to doubt n_e and T_e unless obtained using LTS!

LTS has progressed significantly since the T-3 experiment. There have been three directions in the developments. The first is the TVTS (television Thomson scattering) system developed at PPPL in USA [4]. This system, first installed on PLT and then on TFTR

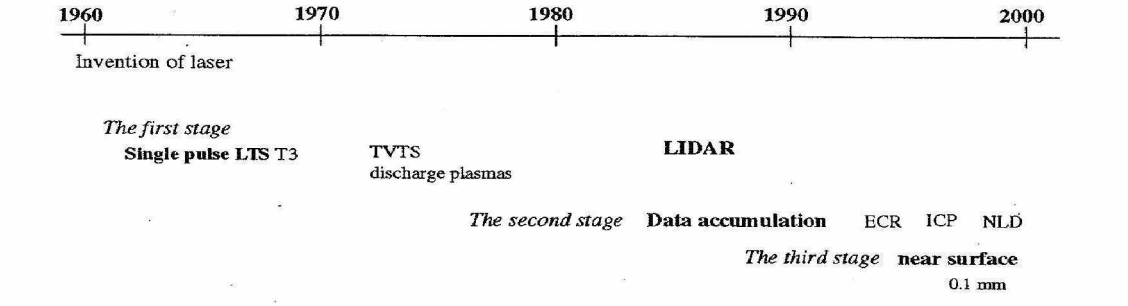

Fig. 1. Three stages of LTS for measurements of electron properties in plasmas

tokamaks, collects scattered signals from many points along the laser beam using a large collection lens and focused onto a multi-channel optical fiber system, which are then sent to a set of spectrometers. In this way, information of n_e and T_e is two-dimensionally displayed against spatial points along the laser beam (thus the term TV). Signals from 74 points along the laser beam could be detected, with a spatial resolution of 10 mm. The second direction is to use a high-repetition YAG laser, developed at Garching in Germany [6]. In this way, temporal developments of n_e and T_e were obtained at a frequency of more than 100 Hz.

The third direction is the LIDAR (light detection and ranging) LTS system, first conceived at Stuttgart University in Germany and jointly developed with JET [5]. This system uses the same window for the laser input and scattered light detection, and the spatial resolution is obtained with the time-of-flight principle using a very short laser pulse and a fast detector. The author had a collaborative work on the LIDAR LTS system to use a streak camera for obtaining a very high spatial resolution [7].

The author has also applied the single-pulse LTS to various DC and pulse discharges [1] in which $n_e > 10^{18}$ m^{-3} [see below in Section 4 for this inequality of n_e]. One example of such measurements is that applied to a discharge pumped excimer laser [8]. Because the duration of the discharge is about 50 ns, one wants to get a temporal resolution of the order of 1 ns. Thus, a laser light from the second harmonic generator (SHG) of a mode-locked YAG laser was used, and the scattered light was dispersed using a double-monochoromator to have a high rejection of stray light and detected using a set of photomultipliers.

Figure 2 is an example of measured spectra, showing the intensity of scattered signals measured at different wavelengths, from a gas mixture of Kr/F/Ne=30 Torr/1.5 Torr/3 atm (a standard gas mix for a KrF laser). The measured spectral points could be fitted with a straight line [on this graph with the abscissa of $(\Delta\lambda)^2$, the wavelength displacement from the laser wavelength squared, against the ordinate of log(signal)] , and this indicates that $f(v_e)$ is a Maxwellian distribution. A numerical simulation of the discharge for these conditions predicted that $f(v_e)$ would be non-Maxwellian distribution. The measurements, however, indicate that $f(v_e)$ be in fact Maxwellian, and so the model used for the simulation was modified to take into account electron-electron collisions, which had been neglected previously. The results of the newer simulation are also shown in Fig. 2 by the thick solid line, and agree satisfactorily with the measurements.

By using this system, temporal developments of n_e and T_e of an excimer laser discharges were measured for the first time, as shown in Fig. 3. It may have been impossible to get this information by other means.

4. THE SECOND STAGE LTS

The Thomson scattered photon number, N_s, is described as

$$N_s = \frac{E_L / S}{h\nu} n_e S' l \sigma_T \Delta\Omega \eta \ , \qquad (1)$$

where E_L is the laser energy, S is the laser beam spot size, $h\nu$ is the photon energy, n_e is the electron density in m^{-3}, $S'l$ is the scattering volume, σ_T is the Thomson cross section per unit solid angle, $\Delta\Omega$ is the solid angle of observation and η is the transmission coefficient.

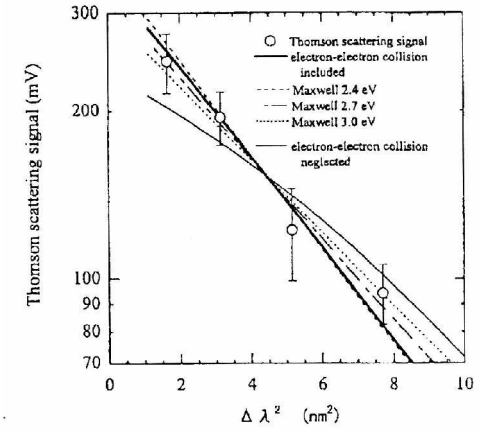

Fig. 2. Thomson scattering spectra for a gas mixture of Kr/F_2/Ne=30 Torr/1.5 Torr/3 atm in a plasma for a discharge-pumped excimer laser

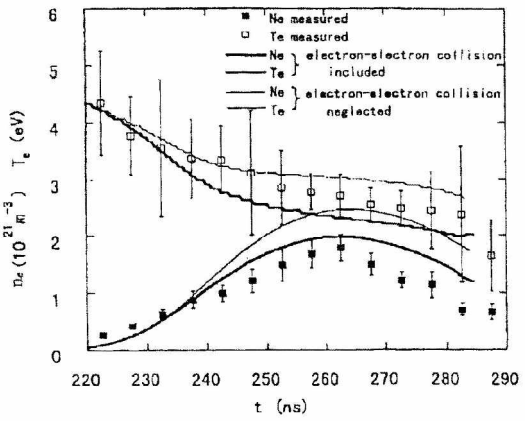

Fig. 3. Temporal evolution of electron temperature T_e and electron density n_e for a gas mixture of Kr/F_2/Ne=30 Torr/1.5 Torr/3 atm in a plasma for a discharge-pumped excimer laser

By inserting appropriate numbers for a typical experimental situation (E_L = 1 J, $h\nu$= 4×10^{-19} J for λ= 500 nm, $S = S'$, l = 0.01 m, σ_T = 9×10^{-30} m^{2}sr^{-1}, $\Delta\Omega$=10^{-3} sr and η = 0.1), one obtains

$$N_s = 2\times10^{-17} n_e \ \text{(photons)}. \qquad (2)$$

There are areas of improvements in the above numbers, such as increases of the laser energy and in the solid angle of observation. However, the quantum efficiency of a photo-detector, such as a photomultiplier, and spectral resolution requirements counter-balance these improvements, and one concludes that $n_e > 10^{18}$ m^{-3} is the minimum detectable electron density for a single- pulse LTS. This is an electron density region typical of high-temperature plasmas and some classes of plasmas for industrial applications, as described in Section 3.

A data accumulation process technique, taking advantage of DC or repetitive operations of some discharges, has been suggested for reducing the limiting electron densities [9]. Such studies have been performed for ECR (electron cyclotron resonance), ICP (induction-coupled plasma) and NLD (neutral-line discharge), and, combined with photon counting, have recently achieved a minimum detectable electron density of 5×10^{15} m^{-3}. Some examples are shown in the following,

which show particular strength of LTS, the data of which are difficult to obtain by other means.

4.1. DEPARTURE FROM MAXWELLIAN *EEDF*

One of the most important aspects of LTS is its capability for making a direct measurement of the eedf. This was exploited to study electron behavior in ICP discharge [10]. To characterize electron behavior in the argon ICP discharge, LTS spectra were measured under various experimental conditions. Figure 4 shows such measurements, measured for various argon gas pressures at the plasma center for an input rf power of 500 W. Because the abscissa and the ordinate are the same as for Fig. 2, the straight line indicates a Gaussian distribution. In this expression, we used the value directly measurable in the spectrometer, but it is to be noted that $(\Delta\lambda)^2 = 10\text{nm}^2$ corresponds to 4.3 eV. Spectra for high pressures do have Gaussian shapes, indicating Maxwellian eedf. At lower pressures, however, the LTS spectra are non-Gaussian, which indicates that the eedfs are non-Maxwellian.

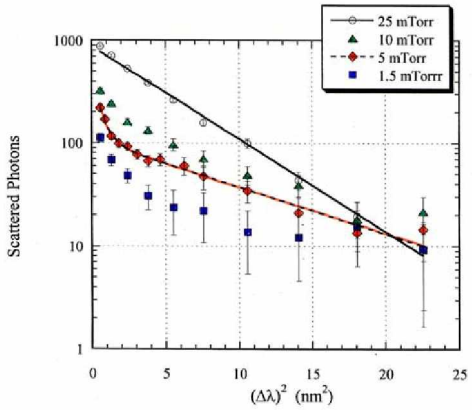

Fig. 4. Thomson scattering spectra from Ar plasmas at various pressures. The measurements were made on an ICP at the plasma center with an input rf power of 500 W

Spatial and temporal distributions were measured for different input powers and pressures, and the temporal changes after switching off the input power were also observed. The results of these measurements are summarized as follows:

(a) The eedfs were clearly non-Maxwellian for some discharge conditions.

(b) These eedfs did not change during the rf cycle. The characteristic times over which the eedfs were observed to change were on the order of microseconds rather than nanoseconds.

(c) The shapes of the eedfs did not vary noticeably with position in the plasma.

Physical interpretations of the observations were discussed in [11].

Recently, this capacity to measure eedfs directly was applied to reactive plasmas. Non-Maxwellian eedfs, similar to those shown in Fig. 4, observed when even small concentrations of CF_4 are present in argon discharges, are attributed to the effect of electron-molecule vibrational excitation collisions [12].

4.2. Bi-MAXWELLIAN *EEDF*

A common feature of many probe studies in low-pressure capacitively coupled rf glow discharges is the observation of a non-Maxwellian eedfs for some discharge conditions. A measured bi-Maxwellian eedf was explained by insufficient energy exchange between the high-temperature component, arising from stochastic electron heating in the rf sheaths, and the low-temperature component formed by being trapped in the central potential well.

In order to confirm this observation, LTS was applied to a capacitively coupled rf glow discharge. Figure 5 shows an LTS spectrum measured at the center of the discharge at an argon pressure of 100 mTorr and an rf power of 40 W [13]. The data were obtained by accumulating scattered signals for 12000 laser shots. It can be seen from the figure that the spectrum is fitted by two straight lines with different slopes, indicating that the eedf for this condition is bi-Maxwellian, with two components of electrons characterized by different temperatures and densities.

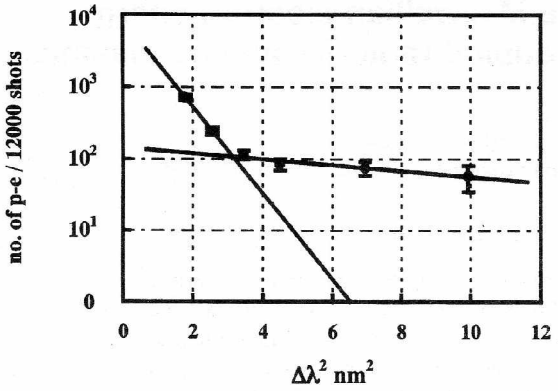

Fig. 5. Thomson scattering spectrum measured on a CCP at the center of the discharge at an Ar pressure of 100 mTorr and an rf power of 40 W with an instrumental half width of a spectrometer of 0.37 nm. The data were accumulated for 12,000 shots

The properties of the two components were determined from the spectrum to be $T_e = (4.6 \pm 1.6)$ eV and $n_e = (1.2 \pm 0.22) \times 10^{16}$ m^{-3} for the high-temperature component, and $T_e = (0.2 \pm 0.02)$ eV and $n_e = (1.76 \pm 0.10) \times \times 10^{17}$ m^{-3} for the low-temperature component. It is to e noted that the monochromator had a reciprocal dispersion of 0.45 nm/mm, and the slit width of 1 mm yielded the measured instrumental width of 0.42 nm FWHM. This value was taken into account to calculate the above temperatures, e.g. $T_e = (0.25 \pm 0.02)$ eV was derived from the Thomson width of 1.26 nm FWHM, which was the deconvolved value of the measured spectral FWHM of 1.30 nm and the above instrumental width.

This and other results provided independent confirmation of the existence of non-Maxwellian eedfs in these discharges for low-pressure conditions. In addition, by adjusting the slit widths of the monochromator used to detect the scattered spectra, we were able to clearly resolve the low energy part of the eedf, which is difficult using probes.

It is to be noted that it was in this low-pressure capacitively coupled rf discharges that the minimum detectable electron density of $n_e = 5 \times 10^{15}$ m^{-3} was obtained [14].

4.3. TEMPERATURE ANISOTROPY

Another strength of LTS is its capability of detecting a temperature anisotropy by simply changing the scattering wave-vector relative to the plasma geometry. An experiment

was carried out to measure velocity distribution function on an ECR system perpendicular and parallel to the magnetic field.

he measured T_e and n_e are plotted for different operating pressures for the ECR plasma in Fig. 6 [15]. These results indicate that n_e increases almost linearly, and T_e decreases first but reaches a constant value, with increasing gas pressure in this pressure range. Also, a temperature anisotropy, detected in the low pressure range for the first time, can be seen in Fig. 6(b).

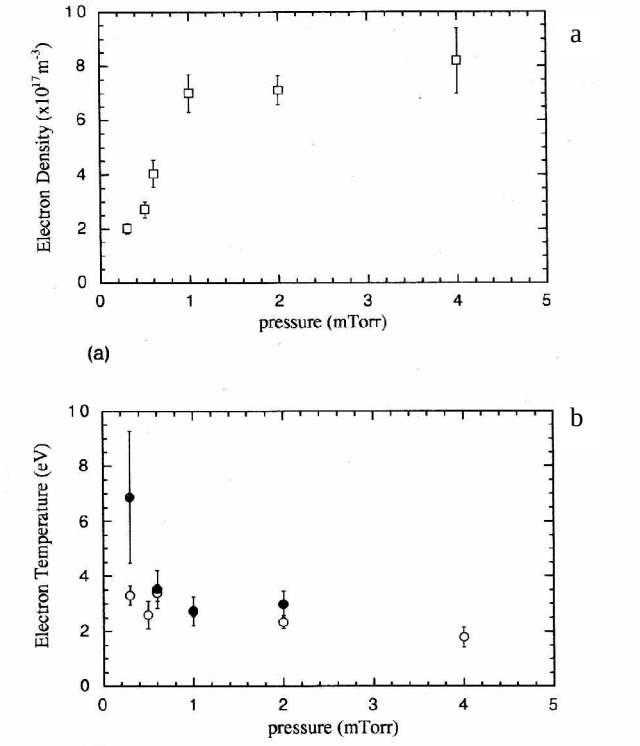

Fig. 6. Electron density (a) and temperature (b) measured as a function of the Ar gas pressure. In (b) the open and closed circles represents temperatures parallel and perpendicular to the magnetic field, respectively

5. THE THIRD STAGE LTS

During the last few years, LTS measurements have been performed on plasmas formed less than 100 μm away from a material surface [16], employing a triple-grating spectrometer having a rejection of above 10^{-8} at 1 nm away from the laser wavelength.

The technique was applied to a micro-discharge simulating a PDP (Plasma Display Panel) discharge. By using appropriate laser powers and working gas mixtures, spatial distributions of T_e and n_e in the range of $-1.0<x<1.5$ mm (x is the coordinate along the electrode surface) were measured at times up to 1.0 μs from application of voltage, where we chose $x=0$ to be at the middle of the electrode gap and $x>0$ for the temporal cathode side. The results are shown in Fig. 7.

Recently, the spatial resolution of measurements has been improved to 60 μm, so that a striation phenomenon, a very prominent feature of this discharge, can now be spatially resolved [17]. Figure 8 shows one of the results. The most remarkable feature of the measurement is that the modulation in T_e is completely out of phase with the modulation in n_e.

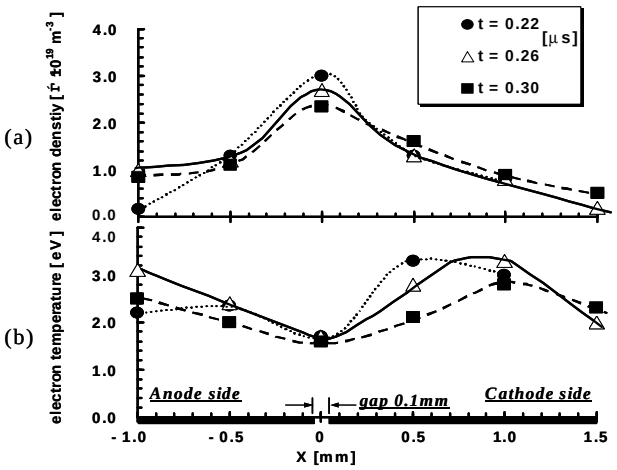

Fig.7. Spatial distributions of electron density n_e (a) and electron temperature T_e (b) at a position of Z=0.1 mm in a discharge simulating a plasma display panel

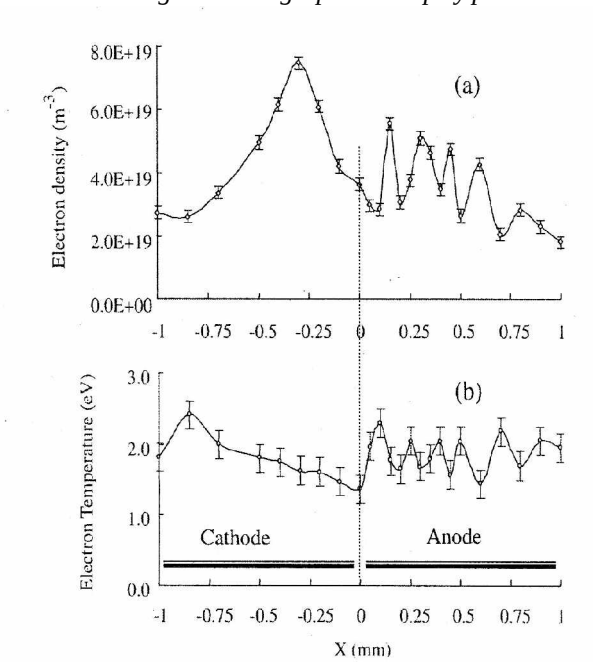

Fig.8. Spatial distributions of electron density n_e (a) and electron temperature T_e (b) of a striated plasma simulating a plasma display panel

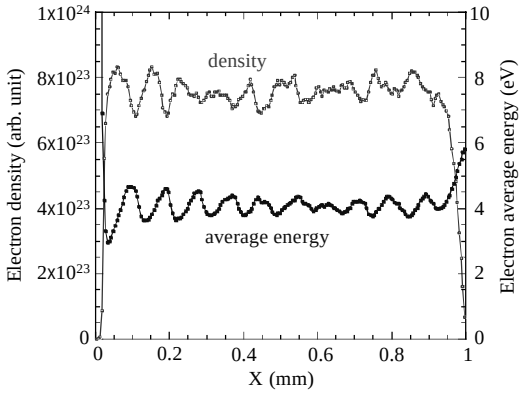

Fig. 9. Spatial distributions of electron density (above) and electron energy (below) of a striated plasma simulating a plasma display panel obtained using a Monte-Carlo numerical simulation

Monte-Carlo simulation has been performed for this discharge condition [18]. Figure 9 illustrates one of such simulations, showing the modulations having the same characteristic as for Fig. 8. This is explained by the sudden deceleration of electrons upon impinging from a cathode fall where the electric field is very high into a positive column where the electric field is weak.

6. SUMMARY

In summarizing the foregoing results and discussion, one concludes that *the first* and *the second stages* LTS are more or less established and routine measurements can be made for any plasma, if conditions are right, such as having sufficient value of n_e and observation environments. Specific environments for LTS measurements may require additional developments, such as LIDAR LTS for ITER divertor plasmas. On the other hand, *the third stage* LTS still needs active developments, aiming at the spatial resolution of 1 μm, an almost diffraction limit for visible lasers. This may open up a possibility of applying LTS into various interesting plasma phenomena, such as studying sheath plasmas very close to electrode surfaces.

ACKNOWLEDGEMENTS

The author wishes to thank those who have contributed various phases of the work described in this article. This work has been supported by a grant from the High-Tech Research Center Establishment Project from the Ministry of Education, Culture, Sports, Science and Technology of Japan.

REFERENCES

1. K. Muraoka and M. Maeda. *Laser-Aided Diagnostics of Plasmas and Gases*. U. K.: IOP Publishing, 2000.
2. K. Muraoka, K. Uchino and M. D. Bowden// *Plasma Phys. Control. Fusion.* 1998, 40, p. 1221.
3. N.J. Peacock, D.C. Robinson, M.J. Forrest, P. Wilcock and V.V. Sannikov// *Nature.* 1968, v.224, p. 448.
4. D. Johnson, D. Dimock, B. Grek, D. Long, D. McNiell, R. Palladino, R. Robinson and E. Tolnas// *Rev. Sci. Instrum.* 1985, v.56, p.1015.
5. H. Salzmann, K Hirsch, P. Nielsen, C. Gowers, Gadd, M. Gadeburg, H. Murmann and A. Schrodter// *Nuclear Fusion.* 1987, v.27, p.1925.
6. H.Roehr, K.-H.Steuer, G.Schramm, K. Hirsch, H. Salzmann// *Nuclear Fusion.* 1982, v.22, p.1099.
7. C. Gowers, H. Fajemirokun, T. Hender, T. Kajiwara, P. Nielsen and B. Schunke// *JET-IR(92)09.* 1992.
8. K. Uchino, Y. Kubo, H. Dozono, H. Yamakoshi, K. Muraoka, M. Maeda, A. Takahashi and M Kato// *Appl. Phys.* 1995, B61, p.165.
9. T. Sakoda, S. Momii, K. Uchino, K.Muraoka, M. D. Bowden, M. Maeda, Y. Manabe, M. Kitagawa and T. Kimura// *Jpn. J. Appl. Phys.* 1991, v.30, L1425.
10. T. Hori, M. D. Bowden, K. Uchino and K. Muraoka// *Appl. Phys.Lett.* 1996, v.69, p.3683.
11. T. Hori, M. D. Bowden, K. Uchino and K. Muraoka// *J. Appl. Phys.* 1998, v.83, p.1909.
12. M. D. Bowden, R. Tabata, P. Suanpoot, K. Uchino, K. Muraoka, M. Noguchi// *J. Appl. Phys.* 2001, v.90, p. 2158.
13. M. Mansour, M. D. Bowden, K. Uchino and K. Muraoka// *Appl. Phys. Lett.* 2001, v.78, p.3187.
14. M. Mansour, M. Koyama, M. D. Bowden, K. Uchino, K. Muraoka// *Jpn. J. Appl. Phys.* 2001, v.40, p.1465.
15. M. D. Bowden, T. Okamoto, F. Kimura, H. Muta, K. Uchino, K. Muraoka, T. Sakoda, M. Maeda, Y. Manabe, M. Kitagawa and T. Kimura// *J. Appl. Phys.* 1993, v.73, p. 2732.
16. Y. Noguchi, Y. Matsuoka, M. D. Bowden, K. Uchino, K. Muraoka// *Jpn. J. Appl. Phys.* 2001, v.40, p.326.
17. S. Hassaballa, K. Tomita, Y. K. Kim, K. Uchino, H. Hatanaka, Y. M. Kim, C. H. Park and K. Muraoka// *Jpn. J. Appl. Phys.* 2005, v.44, L442.
18. K. Muraoka, M. Azumi, K. Suzuki, Y. Yamagata and M. Yagi// *J. Phys.D: Appl. Phys.* 2006, v.39, p.2135.

ДИАГНОСТИКА ПО ЛАЗЕРНОМУ ТОМСОНОВСКОМУ РАССЕЯНИЮ: РАЗВИТИЕ МЕТОДА И ЕГО ИСПОЛЬЗОВАНИЕ ДЛЯ ВЫСОКОТЕМПЕРАТУРНОЙ ПЛАЗМЫ И ПЛАЗМЫ ДЛЯ ПРОМЫШЛЕННЫХ ПРИМЕНЕНИЙ

Кацунори Мураока

Лазерное томсоновское рассеяние начало использоваться для диагностики плазмы почти сразу после изобретения лазера в 1960 г. Наиболее значительный вклад этого метода в развитие физики плазмы и управляемого синтеза был сделан в результате сотрудничества советских и английских физиков, когда в 1968 г. было подтверждено хорошее удержание плазмы в токамаке Т-3. С тех пор интенсивное развитие метода сделало возможным его применение не только для высокотемпературной плазмы, но и для плазмы, используемой в промышленных целях. Представлен краткий обзор развития метода, а также приведены результаты работы автора и рассмотрено их применение для понимания различных плазменных явлений.

ДІАГНОСТИКА ЗА ЛАЗЕРНИМ ТОМСОНОВСЬКИМ РОЗСІЯННЯМ: РОЗВИТОК МЕТОДУ ТА ЙОГО ВИКОРИСТАННЯ ДЛЯ ВИСОКОТЕМПЕРАТУРНОЇ ПЛАЗМИ І ПЛАЗМИ ДЛЯ ПРОМИСЛОВИХ ЗАСТОСУВАНЬ

Кацунорі Мураока

Лазерне томсоновське розсіяння почало використовуватися для діагностики плазми майже відразу після винаходу лазера у 1960 р. Найбільш значний внесок цього методу в розвиток фізики плазми був зроблений в результаті співробітництва радянських і англійських фізиків, коли в 1968 р. було підтверджене добре утримання плазми в токамаку Т-3. Від того часу інтенсивний розвиток методу зробив можливим його застосування не тільки для високотемпературної плазми, але і для плазми, що використовується в промислових цілях. Подається короткий огляд розвитку методу, а також наведені результати роботи автора і розглянуто їх застосування для розуміння різних плазмових явищ.